The Journal of Immunology

Physiologic Thymic Involution Underlies Age-Dependent Accumulation of Senescence-Associated CD4$^+$ T Cells

Kyosuke Sato, Aiko Kato, Miho Sekai, Yoko Hamazaki and Nagahiro Minato

J Immunol published online 24 May 2017
http://www.jimmunol.org/content/early/2017/05/24/jimmunol.1602005

The Journal of Immunology is published twice each month by The American Association of Immunologists, Inc., 1451 Rockville Pike, Suite 650, Rockville, MD 20852

Print ISSN: 0022-1767 Online ISSN: 1550-6606.

Published May 24, 2017, doi:10.4049/jimmunol.1602005

Physiologic Thymic Involution Underlies Age-Dependent Accumulation of Senescence-Associated CD4$^+$ T Cells

Kyosuke Sato, Aiko Kato, Miho Sekai, Yoko Hamazaki, and Nagahiro Minato

Immune aging may underlie various aging-related disorders, including diminished resistance to infection, chronic inflammatory disorders, and autoimmunity. PD-1$^+$ and CD153$^+$ CD44^{high} CD4$^+$ T cells with features of cellular senescence, termed senescence-associated T (SA-T) cells, increasingly accumulate with age and may play a role in the immune aging phenotype. In this article, we demonstrate that, compared with young mice, the aged mouse environment is highly permissive for spontaneous proliferation of transferred naive CD4$^+$ T cells, and it drives their transition to PD-1$^+$ and CD153$^+$ CD44^{high} CD4$^+$ T cells after extensive cell divisions. CD4$^+$ T cells with essentially the same features as SA-T cells in aged mice are also generated from naive CD4$^+$ T cells after extensive cell divisions under severe T-lymphopenic conditions by gamma irradiation or in developmental T cell defect, often in association with spontaneous germinal centers, as seen in aged mice. The increase in SA-T cells is significantly enhanced after thymectomy at the young adult stage, along with accelerated T cell homeostatic proliferation, whereas embryonic thymus implantation in the late adult stage markedly restricts the homeostatic proliferation of naive CD4$^+$ T cells in the host and delays the increase in SA-T cells. Our results suggest that reduced T cell output due to physiologic thymic involution underlies the age-dependent accumulation of SA-T cells as a result of increasing homeostatic proliferation of naive CD4$^+$ T cells. SA-T cells may provide a suitable biomarker of immune aging, as well as a potential target for controlling aging-related disorders. ***The Journal of Immunology*****, 2017, 199: 000–000.**

The thymus shows involution with age in humans and mice, resulting in the progressive decline of T cell output with age (1). The mechanisms underlying the physiologic thymic involution remain controversial and may involve multiple factors, including age-related changes in hematopoietic cells and the thymic microenvironment (2, 3). Although the decrease in thymic organ size becomes evident after adolescence (4), quantitative and qualitative changes in thymic epithelial cells are recognizable much earlier (5, 6). We reported that thymic epithelial cell stem cell activity is rapidly diminished soon after birth, apparently at the cost of robust T cell production during the late fetal and neonatal stages, and it may contribute to the early thymic involution (7–9). The physiologic thymic involution and resulting decrease in T cell output with age should greatly influence the dynamic homeostasis of the peripheral T cell population, although the overall impacts on immune function remain elusive.

Despite the progressive decline in T cell output with age, the overall peripheral T cell population is largely maintained throughout life. However, the T cell population shows a remarkable shift from naive (CD62L^{high} CD44^{low}) to memory (CD62L^{low} CD44^{high}) phenotype with age (10–12). Because Ag-independent, homeostatic proliferation results in phenotypic transition of peripheral naive T cells to memory phenotype in mice (11, 13), the age-dependent shift in the T cell population from naive to memory phenotype may reflect, in part, increasing homeostatic proliferation of peripheral T cells to compensate for diminishing thymic T cell output (12).

A minor subpopulation expressing PD-1 and, to a lesser extent, CD153, is increased in the memory phenotype CD4$^+$ T cells as mice age (10, 14). PD-1$^+$ CD44^{high} CD4$^+$ T cells, in particular those expressing CD153, exhibit features of cellular senescence, such as a marked increase in senescence-related genes (*Cdkn1*, *Cdkn2*) and senescence-associated heterochromatin foci (SAHF), with a profound defect in the Ag-driven proliferation capacity; thus, they are referred to as senescence-associated T (SA-T) cells (14). SA-T cells show additional unique functional features, including biased secretion of abundant proinflammatory cytokines, such as osteopontin (OPN) and chemokines (Ccl3, Ccl4), reminiscent of the SA-secretory phenotype (15), as well as induction of spontaneous germinal centers (GCs) (14). SA-T cells are increased robustly and prematurely in lupus-prone mice and play a crucial role in anti-nuclear autoantibody production and resulting lupus nephritis (13, 15). A recent study reported that SA-T cells also accumulate in visceral adipose tissues under a high-fat diet, causing insulin resistance (16). Thus, SA-T cells may play a role in immune aging phenotypes, such as the decline of acquired immunity, proinflammatory traits, and a higher risk for autoimmunity (17–19). However, the exact mechanism leading to CD4$^+$ T cell senescence remains to be seen.

In the current study, we investigated the possible contribution of physiologic thymic involution to age-dependent accumulation of SA-T cells. We demonstrate that the environment of aged mice is highly permissive for spontaneous, Ag-independent proliferation of

Department of Immunology and Cell Biology, Graduate School of Medicine, Kyoto University, Kyoto 606-8501, Japan

ORCID: 0000-0001-5635-966X (K.S.).

Received for publication November 28, 2016. Accepted for publication April 24, 2017.

This work was supported by Grants-in-Aid from the Ministry of Education, Culture, Sports, Science and Technology of Japan (Scientific Research on Innovative Areas) to N.M. and Y.H.

Address correspondence and reprint requests to Prof. Nagahiro Minato, Department of Immunology and Cell Biology, Graduate School of Medicine, Kyoto University, Yoshida-Konoe-Cho, Sakyo-Ku, Kyoto 606-8501, Japan. E-mail address: minato@imm.med.kyoto-u.ac.jp

The online version of this article contains supplemental material.

Abbreviations used in this article: ATI, thymic implantation at the late adult stage; ATX, thymectomy at the early adult stage; B6, C57BL/6; CTV, CellTrace Violet; E14.5, embryonic day 14.5; GC, germinal center; OPN, osteopontin; SAHF, senescence-associated heterochromatin foci; SA-T, senescence-associated T; STI, sham–thymus-implanted; STX, sham–thymectomy-operated.

naive CD4$^+$ T cells, which eventually lead to the development of SA-T cells via extensive cell division. Thymectomy at the early adult stage (ATX) markedly accelerated the development of SA-T cells, whereas embryonic thymic implantation at the late adult stage (ATI) delayed the accumulation of SA-T cells. Our findings suggest that the age-dependent increase in SA-T cells is an inevitable consequence of continuous homeostatic proliferation of peripheral naive CD4$^+$ T cells due to the progressive decline of thymic T cell output with age.

Materials and Methods

Mice

CD45.2 C57BL/6 (B6) mice were purchased from CLEA Japan (Tokyo, Japan) and Japan SLC (Shizuoka, Japan). CD45.1 mice were purchased from Charles River Laboratories Japan (Kanagawa, Japan). *CD3ε*$^{-/-}$ mice were kindly provided by Dr. S. Fagarasan (RIKEN Center for Integrative Medical Sciences, Kanagawa, Japan). OPN-EGFP knock-in mice were described previously (14). All mice were maintained under specific pathogen–free conditions at the Centre for Experimental Animals of Kyoto University, and the animal experiments were performed in accordance with institutional guidelines.

Flow cytometry

Multicolor flow cytometric analysis and cell sorting were performed using a FACSCanto and FACSAria II/III (BD Biosciences, San Jose, CA), respectively. The following Abs were used: biotin-conjugated anti-CXCR5, PE-conjugated anti-CD121b, CD95, BV421-conjugated streptavidin, and BV510-conjugated anti-CD44 (all from BD Biosciences); biotin-conjugated anti–CD153, FITC-conjugated anti-CD44, anti-Ki67, PE–conjugated streptavidin, and Alexa–eFluor 660–conjugated anti-GL7 (all from eBioscience, San Diego, CA); Alexa Fluor 647–conjugated anti–PD-1, PerCP-Cy5.5–conjugated anti-B220, anti–Mac-1, anti-TER119, allophycocyanin-Cy7–conjugated anti-CD45.1, anti-B220, Pacific Blue–conjugated anti–Mac-1, anti-TER119, and anti-B220 (all from BioLegend, San Diego, CA); PE-Cy7–conjugated anti-CD4 and anti-CD19 (both from Tonbo Biosciences, San Diego, CA); and FITC-conjugated anti-γH2AX (Cell Signaling Technology, Danvers, MA). Propidium iodide (Sigma-Aldrich, St. Louis, MO) or Ghost Dye Violet 450 (Tonbo Biosciences) was used for excluding dead cells. For BrdU staining, the cells were immunostained with PE–anti-CD3 and PerCP-Cy5–anti-CD4, fixed and permeabilized, treated with DNase, and then immunostained with FITC–anti-BrdU (BD Biosciences).

Cell transfer

CD4$^+$ T cells were purified from spleen and lymph node cells from 8-wk-old CD45.1 B6 mice by magnetic-bead depletion with biotin-conjugated CD8a (Tonbo Biosciences), CD11c, CD19, CD49b, CD105, CD117, and PD-1 (all from BD Biosciences), and CD11b, B220, and TER119 (all from BioLegend), as well as anti-biotin beads (Miltenyi Biotec, Bergisch Gladbach, Germany). FACS analysis confirmed that 93–97% of the CD4$^+$ T cell population was CD44^{low} CD62L^{high}. The cells were labeled with CellTrace Violet (CTV; Thermo Fisher Scientific, Waltham, MA), according to the manufacturer's instructions and injected i.v. at 2×10^6 cells per mouse. In some experiments, young and aged mice were kept in the same cages for more than a month before cell transfer.

Immunostaining

Spleens were snap-frozen in optimum cutting temperature compound (Sakura, Torrance, CA), and serial frozen sections were fixed with 95% ethanol and 100% acetone, followed by immunostaining. Abs included anti-B220, anti-CD4, anti–PD-1, anti-CD11c, anti-GL7 (all from BioLegend), and anti-CD3 (BD Biosciences). Immunostained sections were mounted in Mowiol (Calbiochem, La Jolla, CA) and examined under a microscope (Carl Zeiss, Oberkochen, Germany). Tile images of whole-tissue sections were generated using the MosaiX tool in Zeiss AxioVision software (Carl Zeiss). For heterochromatin staining, cells were cytospun, fixed for 10 min in 4% paraformaldehyde, and permeabilized with 0.1% Triton X-100 PBS for 10 min. After blocking, the cells were incubated with anti–HP-1β Ab (Millipore, Billerica, MA), followed by fluorophore Alexa Fluor 488–conjugated secondary Ab and DAPI.

Cytokine assay

OPN in the culture supernatants was assessed by with ELISA kits (cat. no. DY441; R&D Systems, Minneapolis, MN).

Quantitative PCR and single-cell PCR

Quantitative PCR analysis was performed using SYBR Green I Master on a LightCycler 480 Instrument (both from Roche, Basel, Switzerland). Cyclophilin was used as an internal control for mRNA. For single-cell PCR, RNA from single cells sorted with a FACSAria II/III (BD Biosciences) was isolated and amplified on a C1 Single-Cell Auto Prep System (Fluidigm, San Francisco, CA). Quantitative PCR analysis was performed with SsoFast EvaGreen Supermix with Low ROX (PN 172-5211; Bio-Rad, Hercules, CA) on a Biomark HD real-time PCR system (Fluidigm). Hierarchal clustering analysis of the gene expression in single cells was defined based on the Pearson correlation, and heat maps and cluster dendrograms were created with the group average method using R software (version 3.3.1; R Foundation for Statistical Computing, Vienna, Austria). Primer sequences are as follows: *Ascl2*, 5′-GAGAGCTAAGCCCGATGGA-3′ and 5′-AGGTCCACCAGGAGTCACC-3′; *Bcl6*, 5′-TTCCGCTACAAGGGCAAC-3′ and 5′-CAGCGATAGGGTTTCTCACC-3′; *Blimp1*, 5′-TGCGGAGAGGCTCCACTA-3′ and 5′-TGGGTTGCTTTCCGTTTG-3′; *Ccl3*, 5′-TCTGTCACCTGCTCAACATCA-3′ and 5′-CGGGGTGTCAGCTCCATA-3′; *Ccl4*, 5′-AGCAACACCATGAAGCTCTG-3′ and 5′-GAGGGTCAGAGCCCATTG-3′; *Cd30*, 5′-GTCCACGGGAACACCATTT-3′ and 5′-CCAACCAGTAGCACCACCAT-3′; *Cdkn1a*, 5′-AACATCTCAGGGCCGAAA-3′ and 5′-TGCGCTTGGAGTGATAGAAA-3′; *Cdkn1b*, 5′-GTTAGCGGAGCAGTGTCCA-3′ and 5′-TCTGTTCTGTTGGCCCTTTT-3′; *Cdkn2a*, 5′-GGGTTTTCTTGGTGAAGTTCG-3′ and 5′-TTGCCCATCATCATCACCT-3′; *Cdkn2b*, 5′-AATAACTTCCTACGCATTTTCTGC-3′ and 5′-CCCTTGGCTTCAAGGTGAG-3′; *Cebpa*, 5′-AAACAACGCAACGTGGAGA-3′ and 5′-GCGGTCATTGTCACTGGTC-3′; *Cebpb*, 5′-TGATGCAATCCGGATCAA-3′ and 5′-CACGTGTGTTGCGTCAGTC-3′; *Cxcr4*, 5′-TGGAACCGATCAGTGTGAGT-3′ and 5′-GGGCAGGAAGATCCTATTGA-3′; *Cxcr5*, 5′-GAATGACGACAGAGGTTCCTG-3′ and 5′-GCCCAGGTTGGCTTCTTAT-3′; *Ifng*, 5′-ATCTGGAGGAACTGGCAAAA-3′ and 5′-TTCAAGACTTCAAAGAGTCTGAGG-3′; *IL10*, 5′-CAGAGCCACATGCTCCTAGA-3′ and 5′-TGTCCAGCTGGTCCTTTGTT-3′; *Il1r2*, 5′-CCCATCCCTGTGATCATTTC-3′ and 5′-GCACGGGACTATCAGTCTTGA-3′; *Il21*, 5′-TCATCATTGACCTCGTGGCCC-3′ and 5′-ATCGTACTTCTCCACTTGCAATCCC-3′; *Pdcd1*, 5′-CTACCTCTGTGGGGCCATC-3′ and 5′-GAGGTCTCCAGGATTCTCTCTGT-3′; *Ptpn11*, 5′-AGCTGGCTGAGACCACAGAT-3′ and 5′-TGTTGCTGGAGCGTCTCA-3′; *Sostdc1*, 5′-AACAGCACCCTGAATCAAGC-3′ and 5′-CAGCCCACTTGAACTCGAC-3′; *Tbx21*, 5′-CAACCAGCACCAGACAGAGA-3′ and 5′-ACAAACATCCTGTAATGGCTTG-3′; and *Tnfsf8*, 5′-GAGGATCTCTTCTGTACCCTGAAA-3′ and 5′-TTGGTATTGTTGAGATGCTTTGA-3′.

Thymectomy and thymus transplantation

Mice (7–8 wk of age) were anesthetized with pentobarbital, and the thymus was removed with vacuum suction (ATX group). Any mice with detectable thymic remnants at necropsy were excluded from the study. Mice that received a sternum incision under anesthesia without thymic suction (sham operated) were used as the control group. Six or seven whole thymic lobes from embryonic day 14.5 (E14.5) B6 embryos were implanted under the left kidney capsule of B6 mice, as described previously (7). After 3 mo, the mice were sacrificed for multicolor flow cytometric analysis.

BrdU labeling

BrdU (Sigma-Aldrich) was added to the drinking water (0.8 mg/ml) for 9 d before the analysis of ATX and sham-operated mice.

Statistical analyses

Statistical analyses were performed using an unpaired two-tailed Student *t* test and one-way ANOVA with the Bonferroni post hoc test. A p value <0.05 was considered to indicate a significant difference.

Results

Aged mouse environment is highly permissive for spontaneous proliferation of native CD4$^+$ T cells and their phenotypic conversion resembling SA-T cells

We isolated naive CD4$^+$ T cells from the spleen of 2-mo-old CD45.1 B6 mice, labeled them with CTV, and transferred them into young (2-mo-old) or aged (12–20-mo-old) CD45.2 B6 mice with no manipulations. In young recipients, the donor CD4$^+$ T cells showed minimal proliferation in the spleen until 21 d after transfer (Fig. 1A). In contrast, the same donor CD4$^+$ T cells

exhibited robust proliferation in aged mice as early as 5 d after transfer, and nearly 80% of the donor cells, on average, had undergone extensive cell divisions by day 21 (Fig. 1A). FACS analysis revealed that the proportions of PD-1$^+$ CD44^{high} cells were progressively increased in the donor CD4$^+$ T cell progenies in aged recipients, reaching >60% at day 21, whereas most donor T cells remained CD44^{low}, with only 15% being PD-1$^+$ CD44^{high} in young recipients at day 21 (Fig. 1B). The expression of PD-1 in aged recipients was confined to donor T cells that underwent extensive cell divisions (Fig. 1C). A significant fraction of donor-derived PD-1$^+$ CD44^{high} CD4$^+$ T cells in aged recipients also expressed CXCR5 and, to a lesser extent, CD153 and CD121b, essentially similar to host endogenous SA-T cells, although the proportions varied markedly in individual recipients (Fig. 1D). Donor-derived and host CD4$^+$ T cells in young recipients rarely expressed these markers (Fig. 1D). Because homeostatic T cell proliferation can be affected by an altered commensal microbiome in the hosts, we cohoused aged and young mice for more than a month to equalize their microbiomes before cell transfer. Although the aged mice cohoused with young mice again allowed potent naive CD4$^+$ T cell proliferation, donor CD4$^+$ T cells showed minimal proliferation in the young mice cohoused with aged mice, similar to those that were kept alone (Supplemental Fig. 1); this suggests that possible changes in microbiomes with age may play a minimal role, if any, in CD4$^+$ T cell proliferation. The results suggest that naive CD4$^+$ T cells show robust proliferation spontaneously in the aged mouse environment, resulting in phenotypic conversion resembling endogenous SA-T cells.

T cells resembling SA-T cells develop from naive CD4$^+$ T cells as a consequence of extensive homeostatic proliferation under severe T-lymphopenic conditions

To investigate the role of homeostatic proliferation under T-lymphopenic conditions in the characteristic phenotypic conversion of naive CD4$^+$ T cells, we transferred naive CD4$^+$ T cells from CD45.1 B6 mice into young CD45.2 B6 mice irradiated with 5 Gy gamma irradiation. Donor CD4$^+$ T cells exhibited an increase in CD44 expression within a week, and PD-1 expression in the CD44^{high} fraction was markedly increased with a week delay (Fig. 2A). Furthermore, at day 14, significant fractions of donor-derived PD-1$^+$ CD4$^+$ T cells also expressed CXCR5 and CD153, whereas host CD4$^+$ T cells expressed minimal PD-1, with undetectable CXCR5 or CD153, as expected (Fig. 2A, left panels). The numbers of PD-1$^+$ and CD153$^+$ cells increased robustly during the progression of donor T cell proliferation until total CD4$^+$ T cell numbers reached a plateau (Fig. 2A, right panels). A marked increase in CD44 expression, as well as PD-1 and CD153 expression, became detectable only after extensive cell divisions of donor CD4$^+$ T cells (Fig. 2B). In particular, the expression of PD-1 and CD153 was seen only in minor fractions of CTV$^-$ cells, suggesting that the phenotypic conversion occurred only after many rounds of cell divisions much exceeding the detection limit with the CTV dilution. It was noted that CD5 expression also tended to be increased in CTV$^-$ cells (mean fluorescence intensity, 9489 versus 6734 in undivided cells). The expression induction profiles of PD-1 and CD153 were distinct from those in naive CD4$^+$ T cells optimally stimulated with anti-CD3+CD28 Abs, in which PD-1 and CD153 were rapidly induced even before initial cell division and tended to decrease as cell division progressed (Supplemental Fig. 2A). Thus, it seemed unlikely that expression of PD-1 and CD153 during homeostatic proliferation merely reflects transient cell activation. Using *CD3ε*$^{-/-}$ recipients, we confirmed similar generation of PD-1$^+$ and CD153$^+$ cells from transferred naive CD4$^+$ T cells (Fig. 2C). The PD-1$^+$ and CD153$^+$ cells were developed rapidly in 10 d and were sustained significantly for >2 mo, when the total CD4$^+$ T cell numbers reached a plateau (Supplemental Fig. 2B). The results suggest that robust cell divisions during acute homeostatic proliferation of naive CD4$^+$ T cells result in the generation of cells resembling SA-T cells.

PD-1$^+$ and CD153$^+$ CD44^{high} CD4$^+$ T cells generated from naive CD4$^+$ T cells during homeostatic proliferation show a unique gene-expression profile similar to that of SA-T cells

We next compared the transcriptomes of PD-1$^+$ and CD153$^+$ CD44^{high} CD4$^+$ T cells derived from naive CD4$^+$ T cells during acute homeostatic proliferation with those of endogenous SA-T cells in aged mice. PD-1$^+$, and to a greater extent CD153$^+$, CD4$^+$ T cells derived from naive CD4$^+$ T cells in *CD3ε*$^{-/-}$ recipients showed a significant increase in the expression of senescence-related (*Cdkn1a*, *Cdkn2b*) and follicular T cell–related (*Bcl6*, *Cebpa*) genes compared with donor-derived PD-1$^-$ CD4$^+$ T cells, as well as naive CD4$^+$ T cells before transfer, similar to those of freshly isolated SA-T cells from aged mice (Fig. 3A). In addition, PD-1$^+$ and CD153$^+$ CD4$^+$ T cells secreted abundant OPN upon TCR stimulation (Fig. 3A), again similar to SA-T cells (14). Taking advantage of the rapid development of these cells from naive CD4$^+$ T cells in *CD3ε*$^{-/-}$ mice, we investigated the possible expression coordination of diverse genes that are overexpressed in SA-T cells (14), using single-cell RT-PCR analysis. Hierarchal clustering analysis suggested that three groups of genes are induced in a coordinated manner in single cells, including genes related to negative regulation of cell proliferation (*Pdcd1*, *Ptpn11*, *Cdkn1a*, *Cdkn2a*, *Cdkn2b*), inflammation (*Cebpb*, *Blimp1*, *Ccl3*, *Ccl4*, *Ifng*), and follicular T cells (*Bcl6*, *Il21*, *Cxcr5*, *Ascl2*) (Fig. 3B). Notably, the increase in *Tnfsf8* (*Cd153*) was highly coordinated with that of *Ascl2*, which is essential for follicular T cell development (20). Furthermore, these PD-1$^+$ and CD153$^+$ CD4$^+$ T cells that developed from naive CD4$^+$ T cells also showed markedly increased SAHF and γH2AX expression (Fig. 3C, 3D), again similar to SA-T cells in aged mice. Altogether, the findings strongly suggest that a portion of naive CD4$^+$ T cells that have undergone extensive homeostatic proliferation are converted to SA-T cells.

Generation of SA-T cells during homeostatic proliferation is associated with spontaneous GC reaction

Given that SA-T cells are often associated with spontaneous GCs in aged mice (14), we also examined the localization of transferred naive CD4$^+$ T cells in *CD3ε*$^{-/-}$ recipients. Three weeks after transfer of naive CD4$^+$ T cells, the majority of donor T cells were detected diffusely in the follicular regions of the spleen but only minimally in vestigial T cell regions rich in CD11c$^+$ dendritic cells (Fig. 4A, top panels). Among them, PD-1$^+$ T cells were mostly confined to the IgD^{low} region (Fig. 4A, middle panels), which contained abundant GL-7$^+$ cells (Fig. 4A, bottom panels). FACS analysis confirmed that the GL-7$^+$ cells represent CD95$^+$ B cells indicative of GC B cells (Fig. 4B), suggesting that the robust increase in donor PD-1$^+$ T cells was associated with spontaneous GC formation. We previously reported that OPN derived from SA-T cells plays a crucial role in the spontaneous GC reaction (14, 21). Likewise, a minor, yet significant, fraction of PD-1$^+$ CD4$^+$ T cells derived from naive CD4$^+$ T cells from *EGFP-OPN* reporter mice in *CD3ε*$^{-/-}$ recipients showed potent GFP expression, indicative of de novo *Spp1* activation (Fig. 4C). Kinetic analysis indicated that the increase in PD-1$^+$ and CD153$^+$ CD4$^+$ T cells preceded the increase in CD95$^+$ GL-7$^+$ GC B cells by ∼2 wk (Fig. 4C). The results suggest that the robust increase in SA-T cells during acute homeostatic proliferation in follicular regions leads to spontaneous B cell activation and GC formation.

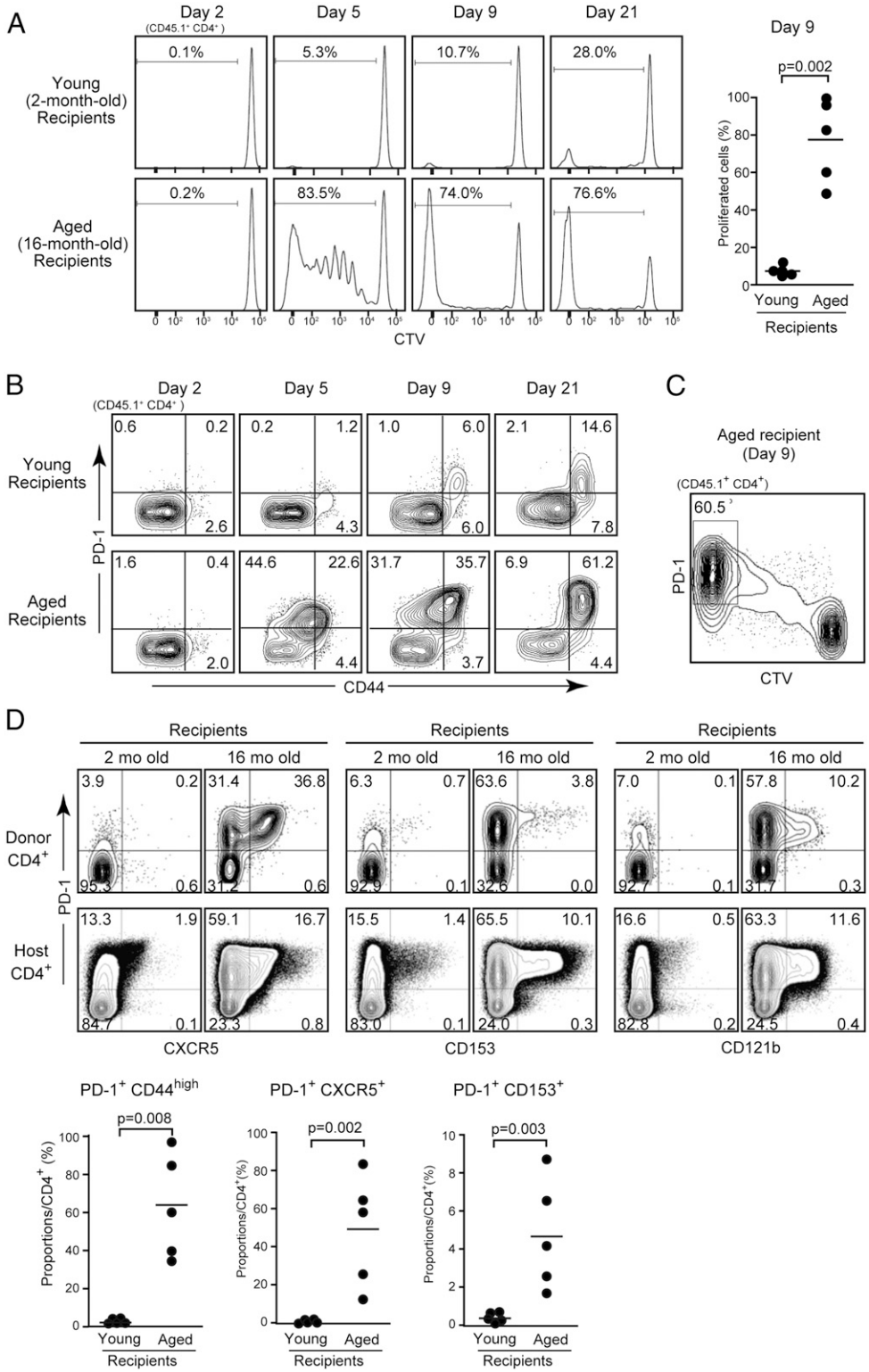

FIGURE 1. Naive CD4$^+$ T cells show robust proliferation in aged, but little proliferation in young, recipients followed by characteristic phenotypic conversion. (**A**–**C**) Naive CD4$^+$ T cells were isolated from 2-mo-old CD45.1 B6 mice, labeled with CTV, and transferred into healthy 2-mo-old (young) and 16-mo-old (aged) CD45.2 B6 mice. At the indicated days after transfer, the spleen cells of recipient mice were analyzed for the expression of CTV in the CD45.1$^+$ CD4$^+$ cell gate. (A) Representative FACS profiles and the proportions of donor-derived CD4$^+$ T cells that underwent cell division at day 9. Expression of PD-1 versus CD44 (B) and PD-1 and CTV (C) in CD45.1$^+$ CD4$^+$ cells in the two recipient groups on the indicated days. (**D**) Nine days after transfer, spleen cells from the two recipient groups were analyzed using multicolor flow cytometry for the expression of the indicated markers in the CD45.1$^+$ (donor) and CD45.2$^+$ (host) CD4$^+$ cell gates (upper panels). The proportions of the indicated cell populations in the CD45.1$^+$ CD4$^+$ cell gates of five mice in two age groups were plotted individually (lower panels). Horizontal lines represent the mean values.

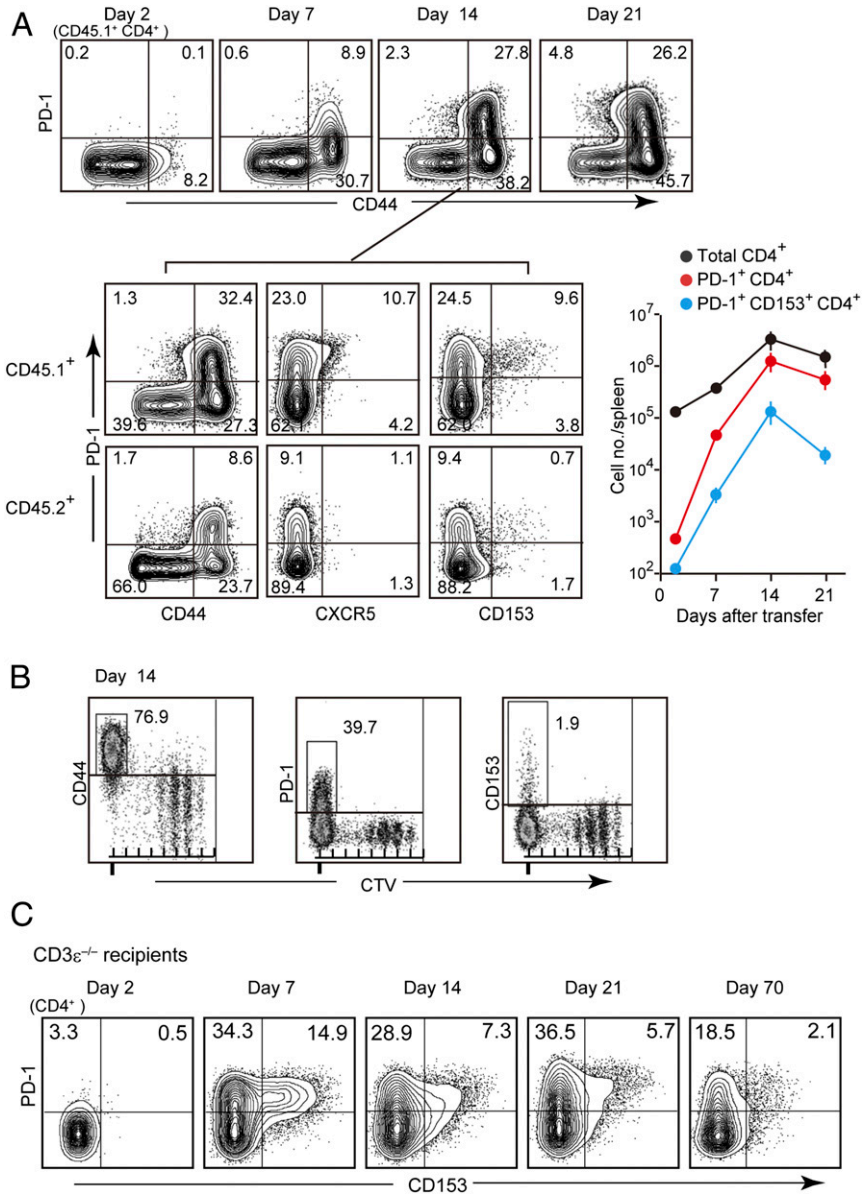

FIGURE 2. Homeostatic proliferation of naive CD4$^+$ T cells under T-lymphopenic conditions results in the phenotypic conversion resembling SA-T cells after numerous rounds of cell division. (**A**) Naive CD4$^+$ T cells were isolated from 2-mo-old CD45.1 B6 mice, labeled with CTV, and transferred into 2-mo-old CD45.2 B6 mice that were subjected to gamma irradiation (5 Gy). At the indicated days after transfer, the spleen cells of recipient mice were analyzed for PD-1 and CD44 expression in the CD45.1$^+$ CD4$^+$ cell gate. At day 14, the spleen cells were analyzed using multicolor flow cytometry for the expression of PD-1 and the indicated markers in the CD45.1$^+$ (donor) and CD45.2$^+$ (host) CD4$^+$ cell gates. The numbers of total CD4$^+$, PD-1$^+$ CD4$^+$, and CD153$^+$ CD4$^+$ cells in the spleen following cell transfer are also shown. Mean and SE of five mice are indicated. (**B**) At day 14, the spleen cells were analyzed for the expression of CD44, PD-1, and CD153 versus CTV in the CD45.1$^+$ CD4$^+$ cell gate. (**C**) Naive CD4$^+$ T cells isolated from 2-mo-old CD45.1 B6 mice were transferred into *CD3ε*$^{-/-}$ mice, and the donor-derived T cells were analyzed for the expression of PD-1 versus CD153 on the indicated days.

Thymectomy at the young adult stage results in the accelerated generation of SA-T cells

To address the impact of thymic involution on the generation of SA-T cells, we examined the effect of ATX at 2 mo of age. ATX mice exhibited a rapid decrease in naive CD4$^+$ T cells in the spleen after ATX that occurred at a greater rate than in sham–thymectomy-operated (STX) mice, whereas memory phenotype CD4$^+$ T cells remained unchanged, resulting in a significant increase in the proportion of memory phenotype cells in the CD4$^+$ T cell population, reminiscent of aged mice (Fig. 5A). When the mice were administered BrdU at 9 d before analysis, ATX mice showed a marked increase in BrdU$^+$ CD4$^+$ T cells, indicating the increased spontaneous proliferation of peripheral CD4$^+$ T cells after ATX (Fig. 5B). Concordantly, the proportions and numbers of PD-1$^+$ and PD-1$^+$ CD153$^+$ CD44^{high} CD4$^+$ T cells were increased in ATX mice compared with STX mice, although the increase in the latter cell numbers barely reached statistical significance because of the very small cell numbers (Fig. 5C, Supplemental Fig. 3). We confirmed that the PD-1$^+$ and CD153$^+$ CD4$^+$ T cell populations that developed in ATX mice exhibited unique gene-expression profiles essentially similar to the corresponding cell fractions in healthy aged mice (Fig. 5D). The results suggest that the decline in thymic function led to the accelerated generation of SA-T cells through increased homeostatic T cell proliferation.

Age-dependent increase in SA-T cells is compromised by ATI

Finally, we addressed whether resuming thymic function at the late adult stage could affect the increase in SA-T cells. To this end, we implanted embryonic (E14.5) thymi (ATI) under the unilateral kidney capsules of B6 mice at the ages of 11–15 mo. ATI mice were sacrificed at 3 mo after the thymic implantation, and those bearing well-developed ectopic thymi with normal T cell–differentiation profiles were subjected to analysis (Fig. 6A, Supplemental Fig. 4A). The proportions of PD-1$^+$ and CD153$^+$ CD44^{high} cells in the splenic CD4$^+$ T cell population were significantly reduced in ATI mice compared with sham–thymus-implanted (STI) mice, whereas those of naive CD4$^+$ T cells were increased (Fig. 6A). To examine whether the effects in ATI mice were related to homeostatic proliferation, we transferred CTV-labeled naive CD4$^+$ T cells from CD45.1 B6 mice into CD45.2 B6 mice that underwent ATI 5 mo prior, at the age of 9 mo (Fig. 6B). ATI mice showed significantly increased CD4$^+$ T cell numbers compared with STI mice

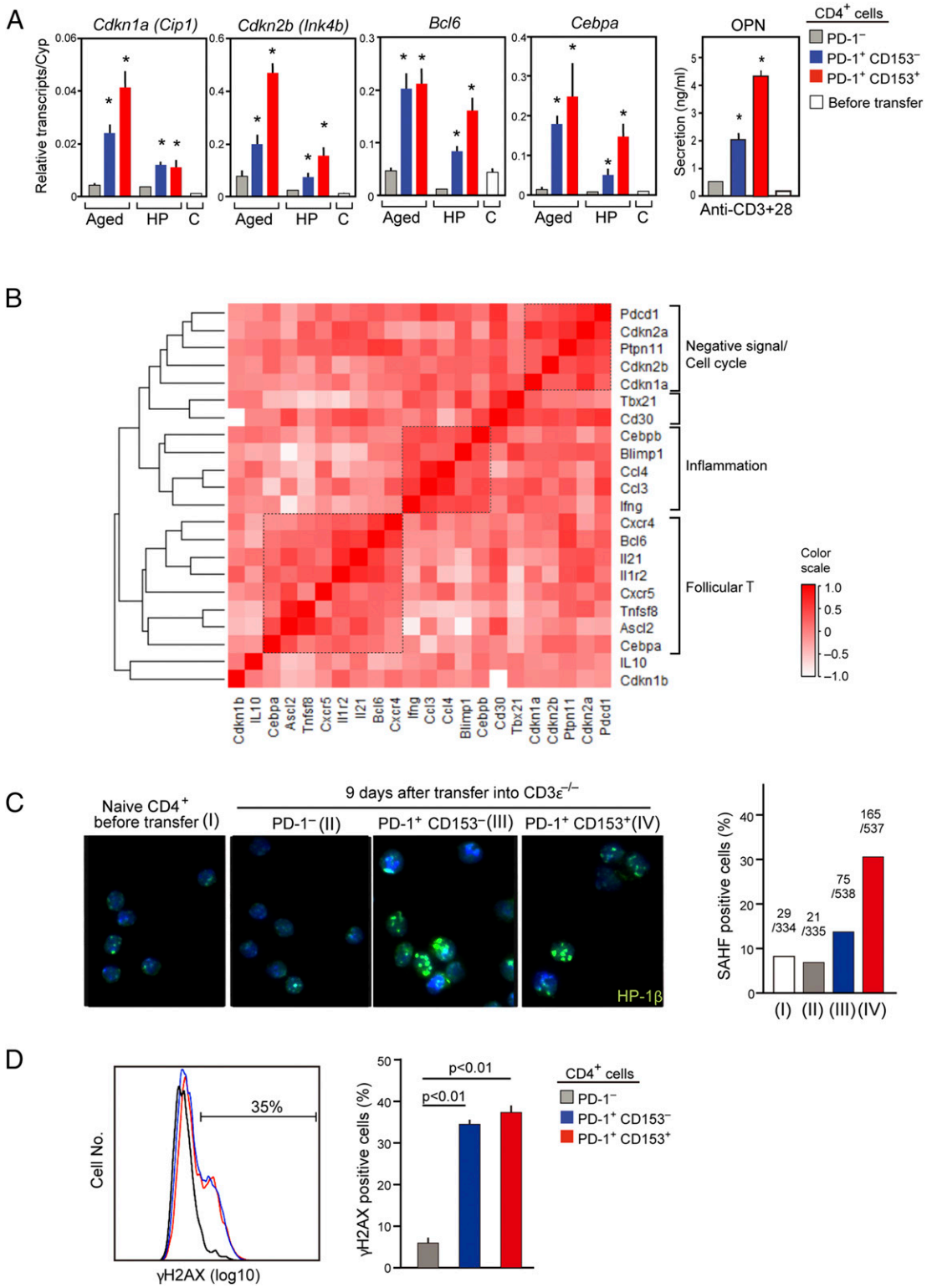

FIGURE 3. PD-1$^+$ and CD153$^+$ CD44^{high} cells derived from naive CD4$^+$ T cells in T-lymphopenic condition show features indistinguishable from those of endogenous SA-T cells in aged mice. (**A**) PD-1$^-$, PD-1$^+$ CD153$^-$, and PD-1$^+$ CD153$^+$ CD44^{high} cells were isolated from 16-mo-old mice (Aged) and from *CD3ε*$^{-/-}$ mice that had been transferred with naive CD4$^+$ T cells 9 d prior (HP). Expression of the transcripts of the indicated genes relative to those of *Cyclophilin* (*Cyp*) was assessed using quantitative RT-PCR. As a control (C), freshly isolated CD44^{low} CD4$^+$ T cells were used. Aliquots of the CD4$^+$ cell subpopulations isolated from *CD3ε*$^{-/-}$ recipients and naive CD4$^+$ T cells before transfer were cultured in the presence of anti-CD3+CD28 Abs for 3 d, and OPN secretion was assessed by ELISA. *$p < 0.05$. (**B**) PD-1$^+$ CD44^{high} CD4$^+$ T cells were sorted from *CD3ε*$^{-/-}$ mice that had been transferred with naive CD4$^+$ T cells 9 d prior and were subjected to single-cell RT-PCR analysis for representative SA-T cell signature genes, and hierarchical cluster analysis was performed. (**C**) PD-1$^-$, PD-1$^+$ CD153$^-$, and PD-1$^+$ CD153$^+$ CD44^{high} CD4$^+$ T cells were isolated from *CD3ε*$^{-/-}$ mice that had been transferred with naive CD4$^+$ T cells 9 d prior and immunostained with DAPI and anti–HP-1β Ab (×200 magnification). Naive CD4$^+$ T cells before transfer were used as a control. Proportions of cells showing more than three distinct SAHF are indicated (numbers per total counted cells). (**D**) Spleen cells from *CD3ε*$^{-/-}$ mice that had been transferred with naive CD4$^+$ T cells 9 d prior were analyzed for γH2AX expression in the indicated gates of the CD4$^+$ T cell subpopulations. Mean γH2AX$^+$ cell populations and SE of three mice are shown.

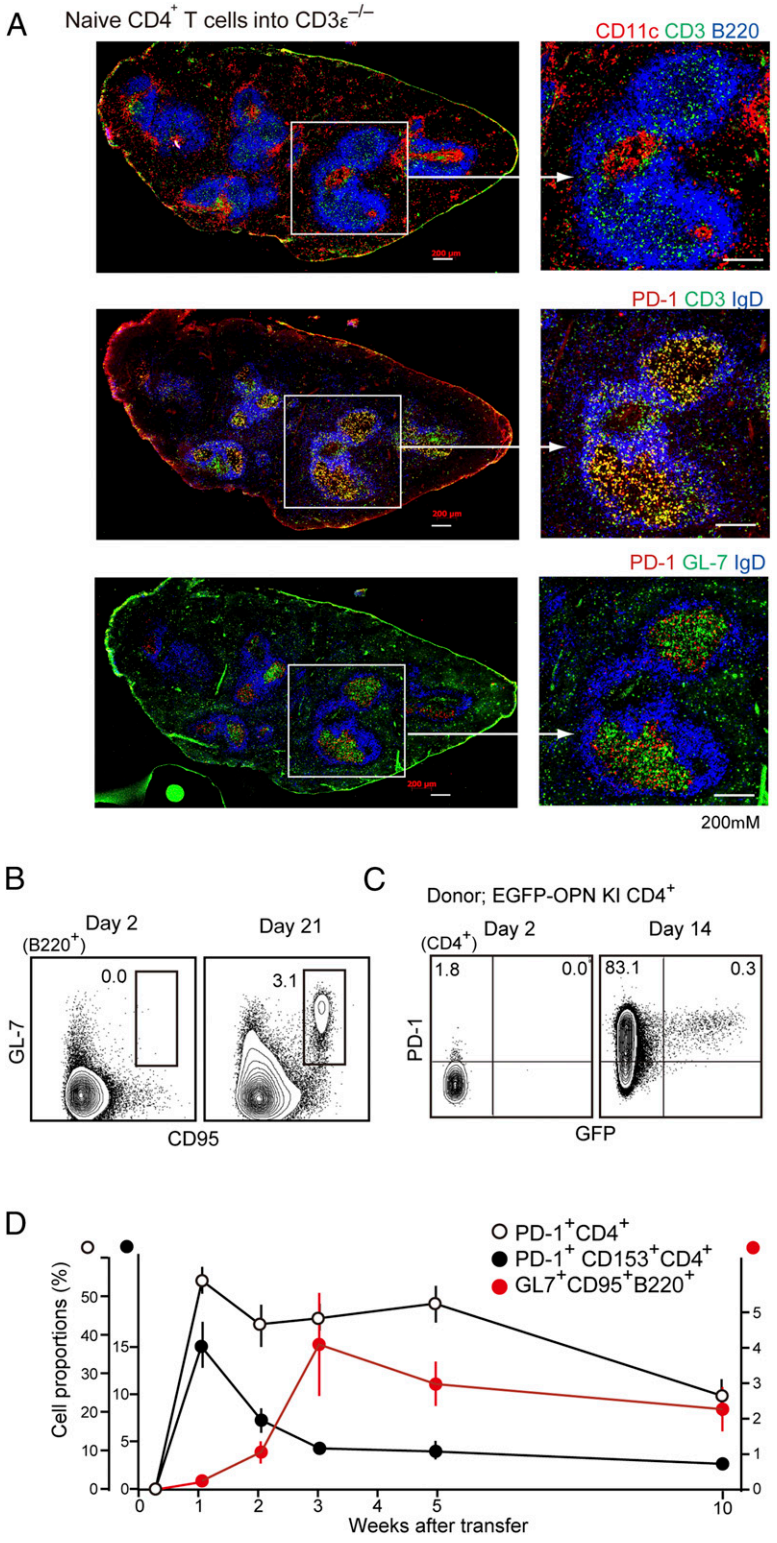

FIGURE 4. SA-T cells generated from naive CD4$^+$ T cells via homeostatic proliferation are associated with spontaneous GC formation. (**A**) Naive CD4$^+$ T cells isolated from 2-mo-old CD45.1 B6 mice were transferred into *CD3ε*$^{-/-}$ mice, and 3 wk later the spleens were multicolor immunostained with the indicated Abs using serial tissue sections. Top, Anti-CD11c (red), anti-CD3 (green), anti-B220 (blue); middle, anti–PD-1 (red), anti-CD3 (green), anti-IgD (blue); bottom, anti-PD-1 (red), anti–GL-7 (green), anti-IgD (blue). Scale bars, 200 μm. (**B**) The spleens of *CD3ε*$^{-/-}$ mice transferred with naive CD4$^+$ T cells 2 and 21 d prior were analyzed for the expression of GL-7 and CD95 in the B220$^+$ cell gate. (**C**) Naive CD4$^+$ T cells isolated from EGFP-OPN reporter mice were transferred into *CD3ε*$^{-/-}$ mice, and the splenic CD4$^+$ T cells were analyzed for PD-1 versus GFP expression at days 2 and 14. (**D**) *CD3ε*$^{-/-}$ mice were transferred with naive CD4$^+$ T cells, and the proportions of PD-1$^+$ and PD-1$^+$ CD153$^+$ CD44^{high} CD4$^+$ T cells of donor origin and GL-7$^+$ CD95$^+$ B220$^+$ (GC) B cells of hosts were assessed at various weeks after cell transfer. The mean and SE of five mice are shown.

(Supplemental Fig. 4B), indicative of resumed T cell output from the ectopic thymi. At day 9 after transfer, donor naive CD4$^+$ T cells exhibited significantly reduced cell proliferation in ATI mice (Fig. 6B). FACS analysis confirmed that the vast majority of donor T cells retained the naive phenotype in ATI recipients, whereas the proportions of naive phenotype cells were variably decreased in STI mice (Fig. 6B). Concordantly, PD-1$^+$ donor T cells were markedly repressed in ATI recipients compared with STI mice; CD153$^+$ donor T cells were quite rare in ATI and STI mice in these experiments (Fig. 6B). These effects paralleled the changes in the CD4$^+$ T cells of the hosts. Thus, host PD-1$^+$ CD44^{high} CD4$^+$ T cells were also reduced significantly, although the decrease in CD153$^+$ CD44^{high} CD4$^+$ T cells was only slight, with no statistical significance (Fig. 6B). The disproportional changes cannot be explained by a mere dilution effect with the increase in naive CD4$^+$ T cells in ATI mice; rather, they may reflect the much longer stability of CD153$^+$ cells than PD-1$^-$ and PD-1$^+$ CD153$^-$ cells (14). To confirm that these effects in ATI mice are due to resumed T cell output, rather than a

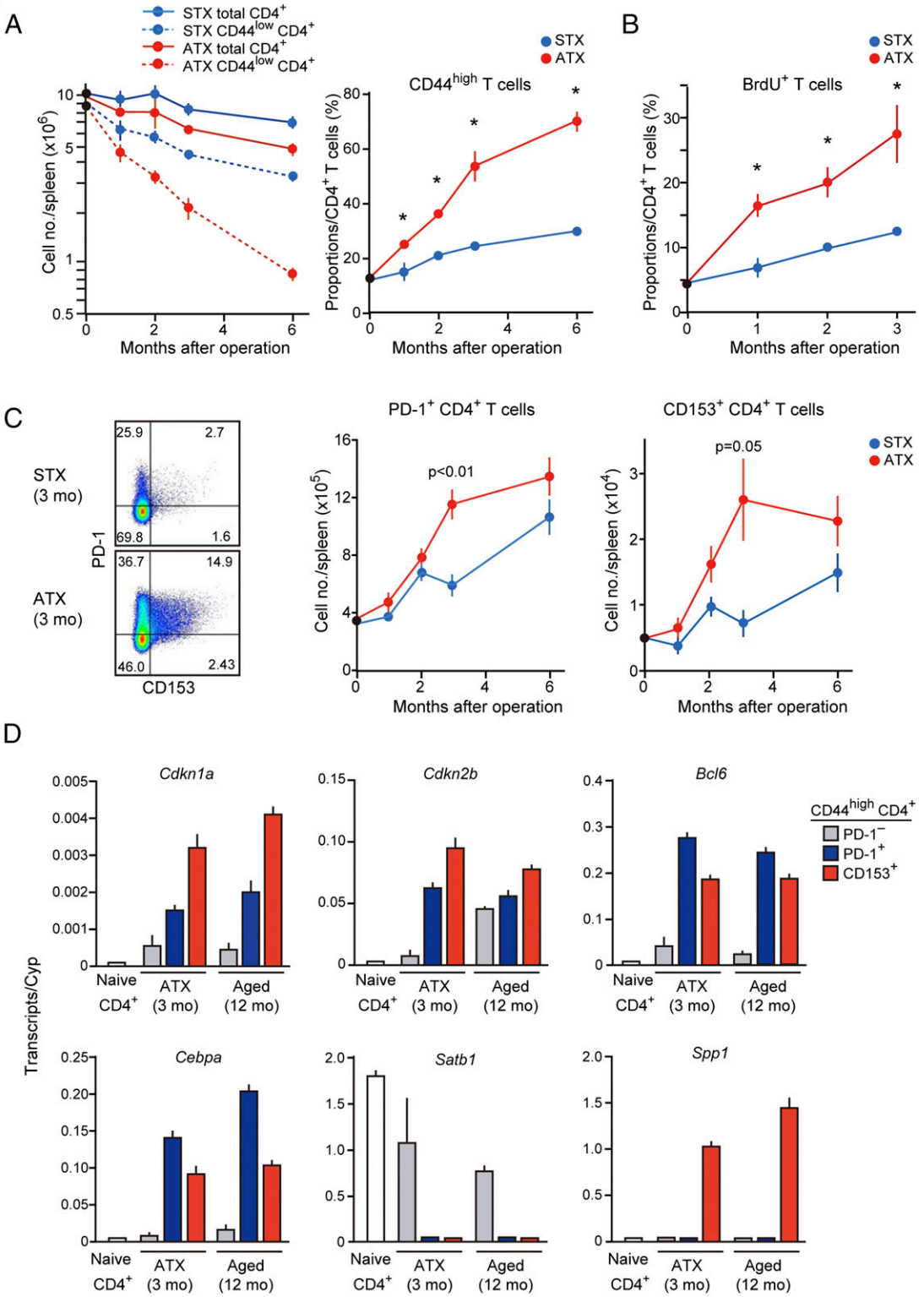

FIGURE 5. Thymectomy at the young adult stage results in the accelerated generation of SA-T cells. (**A**) Two-month-old B6 mice were thymectomized (ATX) or STX, and the numbers of total and CD44^{low} CD4$^+$ T cells in spleen were assessed at the indicated months after operation (left panel). The proportions of CD44^{high} cells in total CD4$^+$ T cells are also shown (right panel). Data represent the mean and SE of three to six mice. (**B**) ATX and STX mice were given BrdU-containing water for 9 d before being sacrificed, and the proportions of BrdU$^+$ cells in CD4$^+$ T cells were analyzed. Data represent the mean and SE of three to six mice. *$p < 0.05$. (**C**) The numbers of PD-1$^+$ CD44^{high} (middle panel) and CD153$^+$ CD44^{high} (right panel) CD4$^+$ T cells in spleens of ATX and STX mice were assessed at the indicated months after surgery. Data represent the mean and SE of three to six mice. Representative FACS profile for PD-1 and CD153 expression in the CD4$^+$ cell gate (left panel). (**D**) PD-1$^-$, PD-1$^+$, and CD153$^+$ CD4$^+$ T cells were purified from 5-mo-old mice that underwent ATX 3 mo prior, as well as from 12-mo-old healthy mice, and were subjected to quantitative RT-PCR for the indicated genes. Naive CD4$^+$ T cells were used as a control. Essentially similar results were obtained in two independent experiments.

functional thymus per se, we continuously transferred naive CD4$^+$ T cells from CD45.1 mice into aged CD45.2 mice and analyzed CD45.2$^+$ CD4$^+$ T cells in the hosts. We found that repetitive transfer of naive CD4$^+$ T cells once a week for 3 mo significantly repressed the increase in host CD153$^+$ SA-T cells (Supplemental Fig. 4C). These results suggest that resumed thymic T cell output at the late adult stage restrains the environmental permissiveness for CD4$^+$ T cell homeostatic proliferation and, thereby, compromises the accumulation of SA-T cells with age.

Discussion

PD-1$^+$ and CD153$^+$ CD44^{high} CD4$^+$ T cells (SA-T cells), which are rarely found in young mice, gradually increase and accumulate as mice age. SA-T cells show characteristic features related to cellular senescence, and the dominance of SA-T cells in the CD4$^+$ T cell population may account, at least in part, for immune aging phenotypes, including diminished acquired immunity, proinflammatory traits, and increasing autoimmunity risk (10, 14, 16, 21).

In the current study, we investigated the physiologic mechanism of the age-dependent increase in SA-T cells. We found that transferred naive CD4$^+$ T cells robustly proliferate in healthy aged mice, but rarely in young mice, and a portion of the progenies that have undergone extensive cell division is eventually converted to cells with features similar to SA-T cells in aged mice. The findings are consistent with our previous observation that the generation of SA-T cells is concordant with an increase in spontaneous CD4$^+$ T cell proliferation with age (14). A recent study indicates that the capacity of homeostatic proliferation of naive T cells following gamma irradiation causing acute lymphopenia is more potent in young mice than in aged mice (22). However, our current findings suggest that, under normal steady-state conditions, the endogenous force driving T cell homeostatic proliferation operates constitutively in the environment of aged mice, whereas it is minimal in that of young mice. We confirmed that T cells resembling SA-T cells in aged mice are robustly developed from naive T cells, even in young mice following gamma irradiation or in *CD3ε*$^{-/-}$ mice through extensive homeostatic proliferation, irrespective of the possible direct driving factors involved. The PD-1$^+$ and, to a greater extent, the CD153$^+$, CD44^{high} CD4$^+$ T cells that developed from naive CD4$^+$ T cells under T lymphopenic conditions in young mice showed a marked increase in senescence-related Cdk-inhibitor genes (*Cdkn1a*, *Cdkn2*), SAHF, and γH2AX, suggestive of replicative cell senescence (23, 24). These T cells also showed increased expression of various proinflammatory genes (*Spp1*, *Ccl3*, *Ccl4*, *Ifng*), reminiscent of the SA-secretory phenotype, and follicular T cell signature genes (*Bcl-6*, *Cebpa*, *Ascl2*, *Cxcr5*, *IL-21*). These features were essentially identical to those of endogenous SA-T cells in aged mice. Notably, it was suggested that the expression of these diverse genes is coordinately induced as functional clusters in individual cells during homeostatic proliferation. In any case, it was suggested that SA-T cells develop as a direct consequence of extensive homeostatic proliferation of naive CD4$^+$ T cells.

Although PD-1 and CD153 are rapidly and transiently expressed by CD4$^+$ T cells with optimal TCR stimulation in a manner independent of the cell cycle, naive CD4$^+$ T cells express PD-1 and CD153 only after extensive rounds of cell division that may far exceed the detection limit with CTV dilution (eight times) during homeostatic proliferation. In cell-transfer experiments with T-lymphopenic mouse models, such extensive cell division of donor naive CD4$^+$ T cells leading to the generation of SA-T cells may be achieved in the early phase of homeostatic proliferation before T cell numbers are restored. However, donor-derived SA-T cells persisted for >2 mo in *CD3ε*$^{-/-}$ mice, suggesting their stability. This may be consistent with much greater stability of SA-T cells compared with naive CD4$^+$ T cells in culture (14). Ag-driven CD4$^+$ T cell proliferation is associated with effector T cell differentiation with a metabolic switch (25). It seems possible that extensive homeostatic proliferation of CD4$^+$ T cells not associated with such a metabolic switch may eventually lead to the cellular senescence. Recent studies indicate that repetitive Ag stimulation in CD8$^+$ T cells during chronic infection also results in the stable expression of PD-1, whose signaling causes the functional exhaustion via metabolic alterations (26, 27). The exhausted Ag-specific CD8$^+$ T cells show a characteristic transcriptome (26), which is apparently distinct from CD4$^+$ SA-T cells (14), and the effects can be reversed by PD-1 signal blockade. In contrast, we reported previously that PD-1 signaling apparently plays no significant role in the generation and function of SA-T cells, because these T cells are similarly increased in *Pd1*$^{-/-}$ mice with age, and the functional features are not reversed by PD-1 blockade (10, 14). Thus, it seems that the overall features of CD4$^+$ SA-T cells reflect cellular senescence associated with extensive cell divisions rather than Ag-driven metabolic exhaustion.

An increasing endogenous force driving peripheral T cell homeostatic proliferation with age may be attributable, at least in part, to the physiologic thymic involution resulting in the age-dependent decline in T cell output (12, 28, 29). In humans, the proportions of proliferating naive phenotype T cells increase progressively with age (30), and this is accelerated in those who underwent thymectomy in early childhood (31). In contrast, in mice, the proliferating T cells with naive phenotype increase slightly with age; thus, it was claimed that peripheral T cell proliferation contributes minimally to the maintenance of naive phenotype T cells (30). However, a remarkable increase in proliferating cells is detected in memory phenotype T cells as mice age (30); thus, the apparent difference may be due, in part, to the rapid conversion of naive T cells to the memory phenotype following homeostatic proliferation in mice but not in humans (32). We confirmed that ATX caused a marked increase in the spontaneous proliferation of CD4$^+$ T cells compared with STX mice. Although naive phenotype CD4$^+$ T cells declined in ATX mice much faster than in STX mice, memory phenotype CD4$^+$ T cell numbers remained the same as those in STX mice for ≥6 mo. Furthermore, PD-1$^+$ and CD153$^+$ T cells in the memory phenotype CD4$^+$ T cells were significantly increased in ATX mice, similar to aged mice. It was confirmed that these T cells show the cell senescence features indistinguishable from SA-T cells in aged mice. The results suggest that thymic involution plays a crucial role in the age-dependent increase in SA-T cells.

An intriguing question is whether the accumulation of endogenous SA-T cells with age can be suppressed by resuming thymic T cell output after the thymic involution. To address the question, we implanted the embryonic thymi at the late adult stage. We found that the environment of aged ATI mice allowed significantly limited homeostatic proliferation of transferred naive CD4$^+$ T cells compared with STI mice; accordingly, we recorded significantly reduced proportions of SA-T cells in ATI mice. Although it is possible that the presence of functional thymus per se limited peripheral T cell proliferation (e.g., via soluble factors), we also found that continuous administration of CD45.1 naive CD4$^+$ T cells to CD45.2 mice suppressed the age-dependent increase in CD45.2 SA-T cells. Together, these results strongly suggest that diminished thymic T cell output due to physiologic thymic involution is a major cause underlying the increase in SA-T cells with age. Our current results indicate that the endogenous force driving the homeostatic proliferation of transferred naive CD4$^+$ T cells is unexpectedly potent in healthy aged mice, and it is conceivable

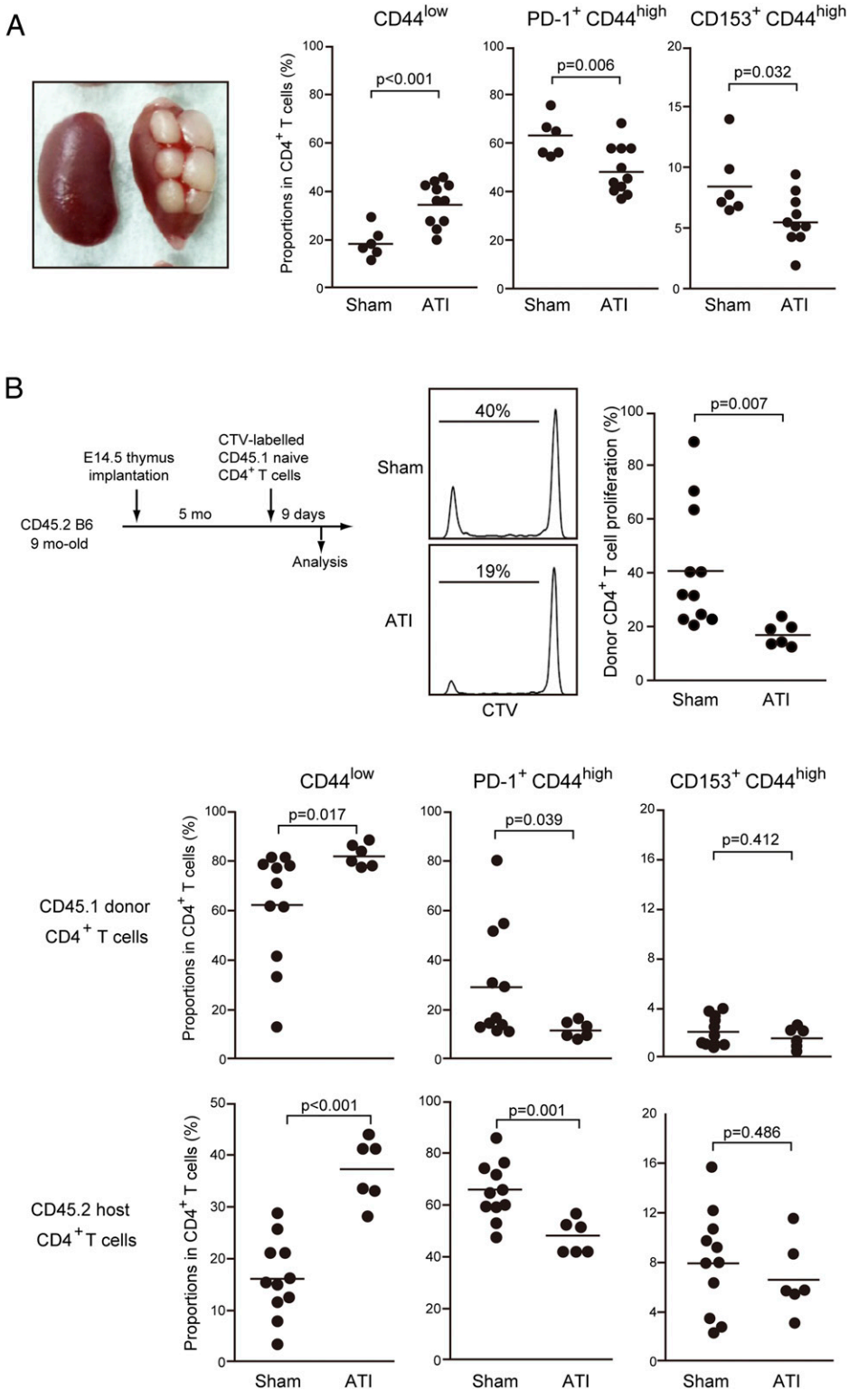

FIGURE 6. Ectopic implantation of the embryonic thymi in aged mice suppresses endogenous $CD4^+$ T cell proliferation and delays the accumulation of SA-T cells. (**A**) Total thymic cells (E14.5) were implanted (ATI) at multiple sites under kidney subcapsules of 11–15-mo-old mice. Control mice underwent the same procedure with no thymic implantation (sham). Three month later, the mice were sacrificed, and spleen cells from mice with well-developed thymic lobes (left panel) were analyzed for the expression of CD44, PD-1, and CD153 in the $CD4^+$ cell gate. The proportions of $CD44^{low}$, PD-1^+ $CD44^{high}$, and $CD153^+$ $CD44^{high}$ cells in individual mice from ATI (6 mice) and sham-operated (11 mice) groups are plotted (three right panels). Horizontal lines represent the mean values. (**B**) Nine-month-old CD45.2 B6 mice were implanted with E14.5 thymic cells (11 mice) or sham operated (6 mice). Five months later, the mice were transferred with naive $CD4^+$ T cells from CD45.1 B6 mice labeled with CTV, and the spleen cells were analyzed for CTV expression in the $CD45.1^+$ $CD4^+$ cell gate. Proportions of cells that underwent at least one cycle of cell division were plotted for individual mice in the ATI and control groups. Horizontal lines represent the mean values. Representative FACS profiles are also shown. The spleen cells were also analyzed for CD44, PD-1, and CD153 expression in the $CD45.1^+$ $CD4^+$ cell gate, and the proportions of the indicated populations in individual mice were plotted. Horizontal lines represent the mean values.

that the sustained homeostatic proliferation in the aged environment leads to the age-dependent increase in SA-T cells.

Homeostatic $CD4^+$ T cell proliferation is driven by tonic TCR signaling via self–MHC class II and homeostatic cytokines (33–36), and this is consistent with the finding that the generation of SA-T cells is dependent on the presence of B cells (14). A recent report indicated that persistent self-antigens play an important role in the selective maintenance of long-lived $CD4^+$ T cells with age (37). As such, sustained homeostatic proliferation may result in the selection of T cells with higher intrinsic TCR affinity for self-antigens (38–42) and may underlie certain overt autoimmune diseases (37, 38). Consistently, T cell populations that underwent homeostatic proliferation showed higher CD5 expression. We reported previously that SA-T cells are robustly increased in the splenic follicular regions of lupus-prone mice, where they secrete abundant OPN in response to autologous B cells and induce spontaneous GC reactions with anti-nuclear Ab production (14, 21). A more recent study indicated that SA-T cells accumulate in

large numbers in visceral fat tissues of mice fed a high-fat diet and cause visceral adiposity with increased insulin resistance (16). In humans, it was reported that the mTOR inhibitor, which delays the onset of various age-related disorders (43), significantly improves influenza vaccination efficacy in the elderly, and the effect is associated with a decrease in peripheral T cells expressing PD-1 (44), although the exact features of the PD-1$^+$ T cells remain to be determined. Thus, it is an intriguing possibility that the increasing dominance of SA-T cells in the peripheral T cell population with age plays a part in the development of various age-related disorders, including diminished acquired immunity, proinflammatory traits, and increased autoimmunity risk.

Although physiologic thymic involution that begins early in life strongly affects the homeostatic dynamics of the peripheral T cell population throughout the lifespan, its possible impact on overall immune function has remained controversial. Our current results indicate that thymic involution underlies the age-dependent increase in SA-T cells. The extent of immune aging may vary significantly elderly individuals, and SA-T cells may serve as a suitable biomarker for immune aging and a potential target controlling the disorders related to immune aging in humans.

Acknowledgments

We thank Dr. Sidonia Fagarasan for providing *CD3ε*$^{-/-}$ mice.

Disclosures

The authors have no financial conflicts of interest.

References

1. Palmer, D. B. 2013. The effect of age on thymic function. *Front. Immunol.* 4: 316.
2. Chinn, I. K., C. C. Blackburn, N. R. Manley, and G. D. Sempowski. 2012. Changes in primary lymphoid organs with aging. *Semin. Immunol.* 24: 309–320.
3. Lynch, H. E., G. L. Goldberg, A. Chidgey, M. R. M. Van den Brink, R. Boyd, and G. D. Sempowski. 2009. Thymic involution and immune reconstitution. *Trends Immunol.* 30: 366–373.
4. Jamieson, B. D., D. C. Douek, S. Killian, L. E. Hultin, D. D. Scripture-Adams, J. V. Giorgi, D. Marelli, R. A. Koup, and J. A. Zack. 1999. Generation of functional thymocytes in the human adult. *Immunity* 10: 569–575.
5. Immunological Genome Consortium. 2013. The transcriptional landscape of αβ T cell differentiation. *Nat. Immunol.* 14: 619–632.
6. Shanley, D. P., D. Aw, N. R. Manley, and D. B. Palmer. 2009. An evolutionary perspective on the mechanisms of immunosenescence. *Trends Immunol.* 30: 374–381.
7. Sekai, M., Y. Hamazaki, and N. Minato. 2014. Medullary thymic epithelial stem cells maintain a functional thymus to ensure lifelong central T cell tolerance. *Immunity* 41: 753–761.
8. Hamazaki, Y., M. Sekai, and N. Minato. 2016. Medullary thymic epithelial stem cells: role in thymic epithelial cell maintenance and thymic involution. *Immunol. Rev.* 271: 38–55.
9. Hamazaki, Y. 2015. Adult thymic epithelial cell (TEC) progenitors and TEC stem cells: models and mechanisms for TEC development and maintenance. *Eur. J. Immunol.* 45: 2985–2993.
10. Shimatani, K., Y. Nakashima, M. Hattori, Y. Hamazaki, and N. Minato. 2009. PD-1+ memory phenotype CD4+ T cells expressing C/EBPalpha underlie T cell immunodepression in senescence and leukemia. *Proc. Natl. Acad. Sci. USA* 106: 15807–15812.
11. Sprent, J., and C. D. Surh. 2011. Normal T cell homeostasis: the conversion of naive cells into memory-phenotype cells. *Nat. Immunol.* 12: 478–484.
12. Goronzy, J. J., and C. M. Weyand. 2005. T cell development and receptor diversity during aging. *Curr. Opin. Immunol.* 17: 468–475.
13. Goldrath, A. W., L. Y. Bogatzki, and M. J. Bevan. 2000. Naive T cells transiently acquire a memory-like phenotype during homeostasis-driven proliferation. *J. Exp. Med.* 192: 557–564.
14. Tahir, S., Y. Fukushima, K. Sakamoto, K. Sato, H. Fujita, J. Inoue, T. Uede, Y. Hamazaki, M. Hattori, and N. Minato. 2015. A CD153+CD4+ T follicular cell population with cell-senescence features plays a crucial role in lupus pathogenesis via osteopontin production. *J. Immunol.* 194: 5725–5735.
15. Freund, A., A. V. Orjalo, P.-Y. Desprez, and J. Campisi. 2010. Inflammatory networks during cellular senescence: causes and consequences. *Trends Mol. Med.* 16: 238–246.
16. Shirakawa, K., X. Yan, K. Shinmura, J. Endo, M. Kataoka, Y. Katsumata, T. Yamamoto, A. Anzai, S. Isobe, N. Yoshida, et al. 2016. Obesity accelerates T cell senescence in murine visceral adipose tissue. *J. Clin. Invest.* 126: 4626–4639.
17. Goronzy, J. J., and C. M. Weyand. 2013. Understanding immunosenescence to improve responses to vaccines. *Nat. Immunol.* 14: 428–436.
18. Franceschi, C., and J. Campisi. 2014. Chronic inflammation (inflammaging) and its potential contribution to age-associated diseases. *J. Gerontol. A Biol. Sci. Med. Sci.* 69(Suppl. 1): S4–S9.
19. Loeser, R. F., J. A. Collins, and B. O. Diekman. 2016. Ageing and the pathogenesis of osteoarthritis. *Nat. Rev. Rheumatol.* 12: 412–420.
20. Liu, X., X. Chen, B. Zhong, A. Wang, X. Wang, F. Chu, R. I. Nurieva, X. Yan, P. Chen, L. G. van der Flier, et al. 2014. Transcription factor achaete-scute homologue 2 initiates follicular T-helper-cell development. *Nature* 507: 513–518.
21. Sakamoto, K., Y. Fukushima, K. Ito, M. Matsuda, S. Nagata, N. Minato, and M. Hattori. 2016. Osteopontin in spontaneous germinal centers inhibits apoptotic cell engulfment and promotes anti-nuclear antibody production in lupus-prone mice. *J. Immunol.* 197: 2177–2186.
22. Becklund, B. R., J. F. Purton, C. Ramsey, S. Favre, T. K. Vogt, C. E. Martin, D. S. Spasova, G. Sarkisyan, E. LeRoy, J. T. Tan, et al. 2016. The aged lymphoid tissue environment fails to support naïve T cell homeostasis. *Sci. Rep.* 6: 30842.
23. Narita, M., S. Nũnez, E. Heard, M. Narita, A. W. Lin, S. A. Hearn, D. L. Spector, G. J. Hannon, and S. W. Lowe. 2003. Rb-mediated heterochromatin formation and silencing of E2F target genes during cellular senescence. *Cell* 113: 703–716.
24. Nakamura, A. J., C. E. Redon, W. M. Bonner, and O. A. Sedelnikova. 2009. Telomere-dependent and telomere-independent origins of endogenous DNA damage in tumor cells. *Aging (Albany NY)* 1: 212–218.
25. Buck, M. D., D. O'Sullivan, and E. L. Pearce. 2015. T cell metabolism drives immunity. *J. Exp. Med.* 212: 1345–1360.
26. Bengsch, B., A. L. Johnson, M. Kurachi, P. M. Odorizzi, K. E. Pauken, J. Attanasio, E. Stelekati, L. M. McLane, M. A. Paley, G. M. Delgoffe, and E. J. Wherry. 2016. Bioenergetic insufficiencies due to metabolic alterations regulated by the inhibitory receptor PD-1 are an early driver of CD8(+) T cell exhaustion. *Immunity* 45: 358–373.
27. Balmer, M. L., and C. Hess. 2016. Feeling worn out? PGC1α to the rescue for dysfunctional mitochondria in T cell exhaustion. *Immunity* 45: 233–235.
28. Mitchell, W. A., P. O. Lang, and R. Aspinall. 2010. Tracing thymic output in older individuals. *Clin. Exp. Immunol.* 161: 497–503.
29. Grubeck-Loebenstein, B., and G. Wick. 2002. The aging of the immune system. *Adv. Immunol.* 80: 243–284.
30. den Braber, I., T. Mugwagwa, N. Vrisekoop, L. Westera, R. Mögling, A. B. de Boer, N. Willems, E. H. Schrijver, G. Spierenburg, K. Gaiser, et al. 2012. Maintenance of peripheral naive T cells is sustained by thymus output in mice but not humans. *Immunity* 36: 288–297.
31. Prelog, M., M. Keller, R. Geiger, A. Brandstätter, R. Würzner, U. Schweigmann, M. Zlamy, L. B. Zimmerhackl, and B. Grubeck-Loebenstein. 2009. Thymectomy in early childhood: significant alterations of the CD4(+)CD45RA(+)CD62L(+) T cell compartment in later life. *Clin. Immunol.* 130: 123–132.
32. Surh, C. D., and J. Sprent. 2008. Homeostasis of naive and memory T cells. *Immunity* 29: 848–862.
33. Goldrath, A. W., and M. J. Bevan. 1999. Selecting and maintaining a diverse T-cell repertoire. *Nature* 402: 255–262.
34. Wu, Z., S. J. Bensinger, J. Zhang, C. Chen, X. Yuan, X. Huang, J. F. Markmann, A. Kassaee, B. R. Rosengard, W. W. Hancock, et al. 2004. Homeostatic proliferation is a barrier to transplantation tolerance. *Nat. Med.* 10: 87–92.
35. Gudmundsdottir, H., and L. A. Turka. 2001. A closer look at homeostatic proliferation of CD4+ T cells: costimulatory requirements and role in memory formation. *J. Immunol.* 167: 3699–3707.
36. Takada, K., and S. C. Jameson. 2009. Naive T cell homeostasis: from awareness of space to a sense of place. *Nat. Rev. Immunol.* 9: 823–832.
37. Zhang, B., Q. Jia, C. Bock, G. Chen, H. Yu, Q. Ni, Y. Wan, Q. Li, and Y. Zhuang. 2016. Glimpse of natural selection of long-lived T-cell clones in healthy life. *Proc. Natl. Acad. Sci. USA* 113: 9858–9863.
38. Ernst, B., D.-S. Lee, J. M. Chang, J. Sprent, and C. D. Surh. 1999. The peptide ligands mediating positive selection in the thymus control T cell survival and homeostatic proliferation in the periphery. *Immunity* 11: 173–181.
39. Baccala, R., and A. N. Theofilopoulos. 2005. The new paradigm of T-cell homeostatic proliferation-induced autoimmunity. *Trends Immunol.* 26: 5–8.
40. Kassiotis, G., R. Zamoyska, and B. Stockinger. 2003. Involvement of avidity for major histocompatibility complex in homeostasis of naive and memory T cells. *J. Exp. Med.* 197: 1007–1016.
41. Kieper, W. C., J. T. Burghardt, and C. D. Surh. 2004. A role for TCR affinity in regulating naive T cell homeostasis. *J. Immunol.* 172: 40–44.
42. Calzascia, T., M. Pellegrini, A. Lin, K. M. Garza, A. R. Elford, A. Shahinian, P. S. Ohashi, and T. W. Mak. 2008. CD4 T cells, lymphopenia, and IL-7 in a multistep pathway to autoimmunity. *Proc. Natl. Acad. Sci. USA* 105: 2999–3004.
43. Wilkinson, J. E., L. Burmeister, S. V. Brooks, C.-C. Chan, S. Friedline, D. E. Harrison, J. F. Hejtmancik, N. Nadon, R. Strong, L. K. Wood, et al. 2012. Rapamycin slows aging in mice. *Aging Cell* 11: 675–682.
44. Mannick, J. B., G. Del Giudice, M. Lattanzi, N. M. Valiante, J. Praestgaard, B. Huang, M. A. Lonetto, H. T. Maecker, J. Kovarik, S. Carson, et al. 2014. mTOR inhibition improves immune function in the elderly. *Sci. Transl. Med.* 6: 268ra179.

Supplementary Figures

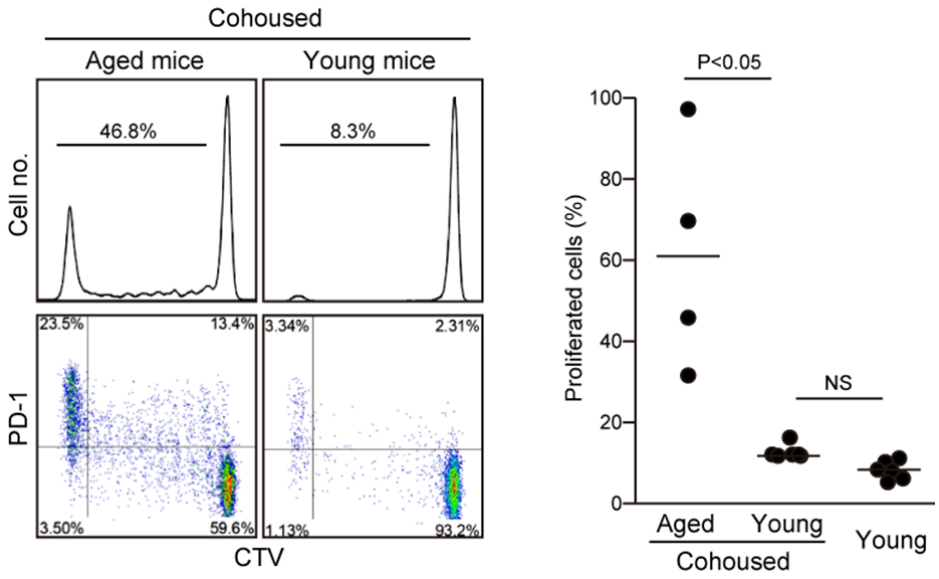

Fig. S1. Young mice cohoused with aged mice hardly allow the spontaneous proliferation of naïve $CD4^+$ T cells. Young (2-month old) and elder (1 year old) CD45.2 B6 mice were cohoused for more than a month, and then they were transferred with CTV-labeled naïve $CD4^+$ T cells from CD45.1 B6 mice. Nine day after transfer, the splenic cells were analyzed for PD-1 and CTV expression at the gate of $CD45.1^+$ $CD4^+$ cells. The proportions of donor $CD4^+$ cells that proliferated at least once are plotted.

A

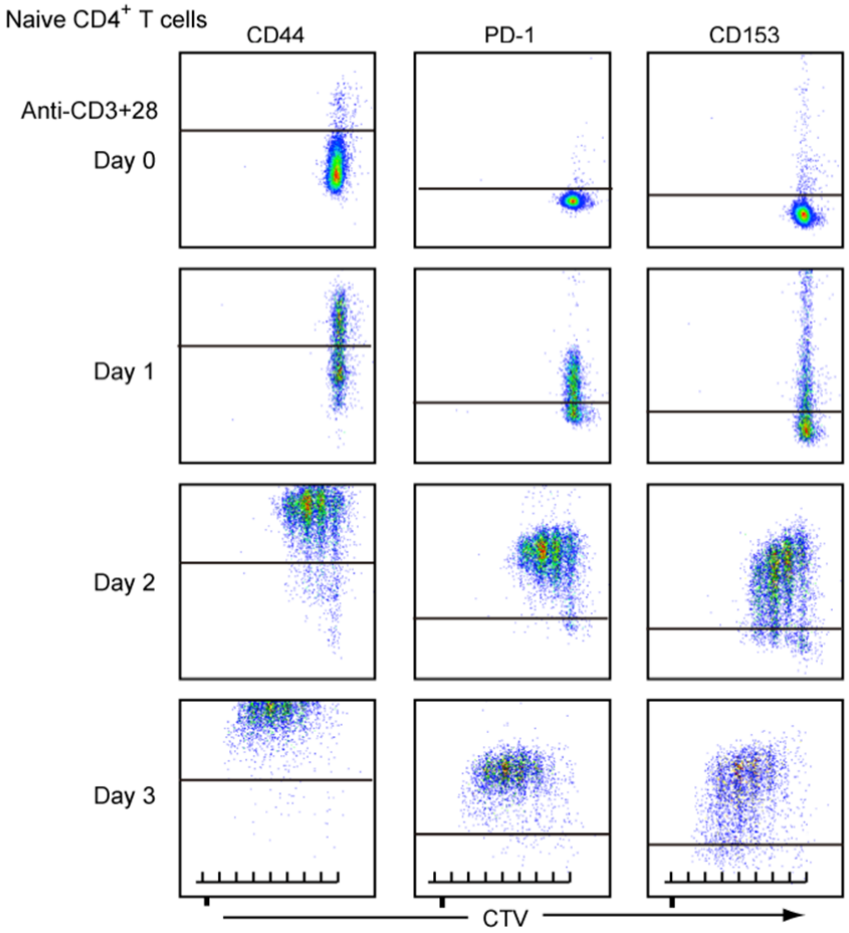
Naive CD4+ T cells
CD44
PD-1
CD153
Anti-CD3+28
Day 0
Day 1
Day 2
Day 3
CTV

B

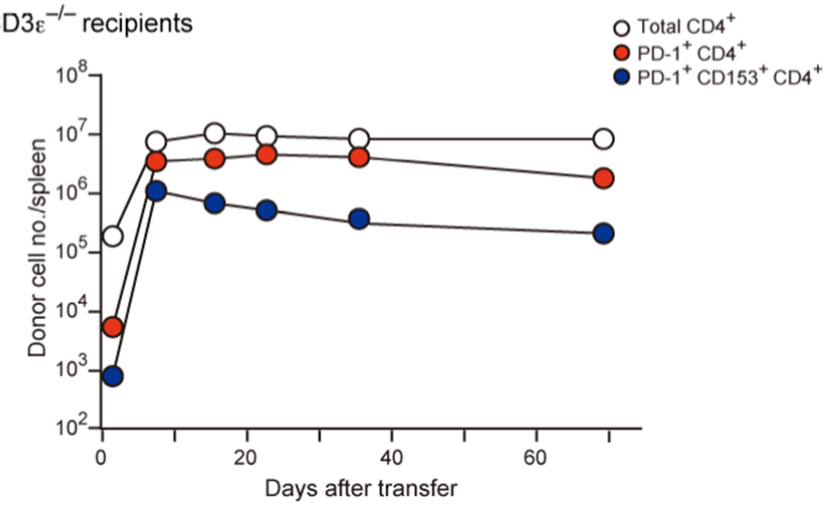
CD3ε−/− recipients
Total CD4+
PD-1+ CD4+
PD-1+ CD153+ CD4+
Donor cell no./spleen
10^8
10^7
10^6
10^5
10^4
10^3
10^2
0
20
40
60
Days after transfer

Fig. S2. (**A**) Rapid expression of CD44, PD-1, and CD153 in naïve $CD4^+$ T cells independent of cell cycles via optimal TCR-stimulation. Freshly isolated $CD44^{low}$ $CD4^+$ T cells were labeled with CTV and cultured in the presence of anti-CD3 + CD28 for indicated periods, followed by FACS analysis for indicated antibody vs. CTV. (**B**) $PD\text{-}1^+$ and $CD153^+$ cells are rapidly generated from naïve $CD4^+$ T cells in $CD3\varepsilon^{-/-}$ recipients and sustained for more than 2 months.

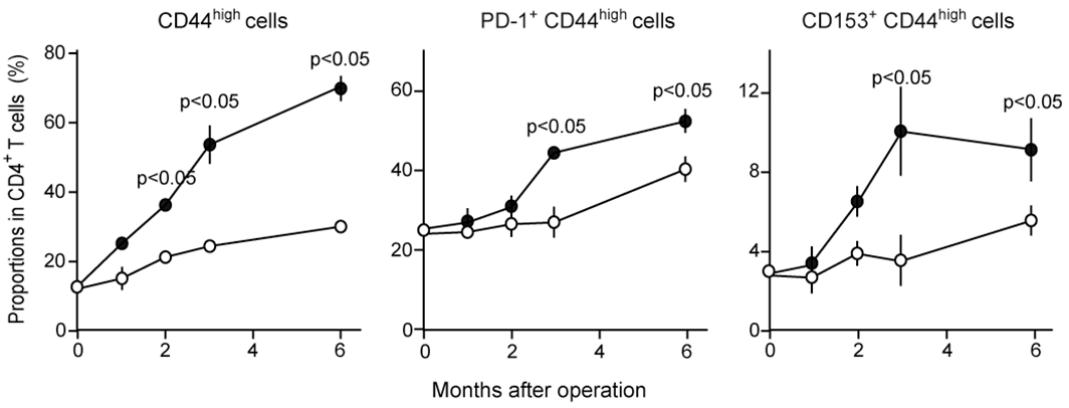

Fig. S3. Increase in the proportions of PD-1^{+} and CD153^{+} CD4^{+} T cells after ATX at young stage. B6 mice received ATX (solid circles) or sham operation (open circles) at 2 months of age, and the proportions of CD22^{high}, PD-1^{+} and CD153^{+} CD4^{+} T cells were assessed at indicated periods after the operation.

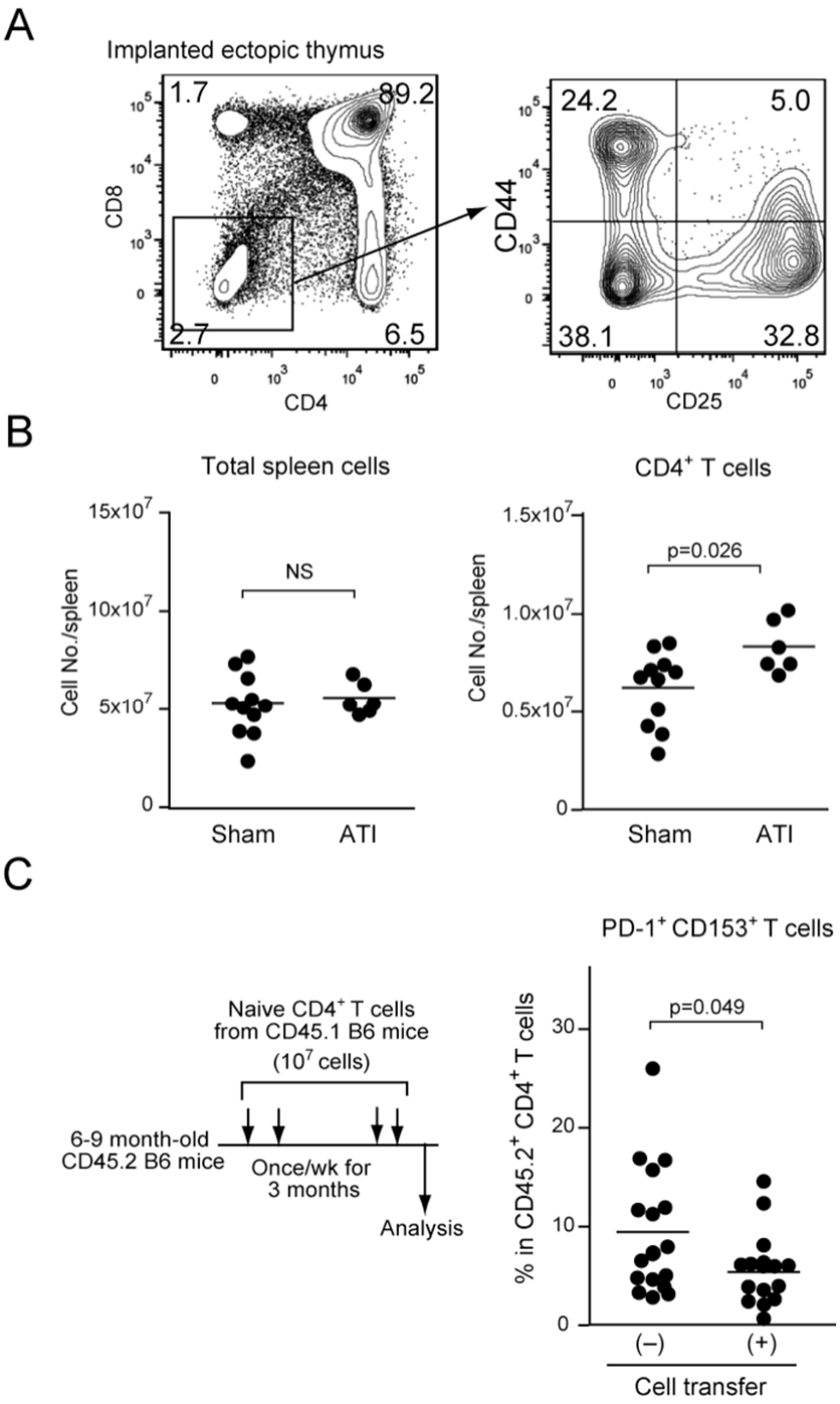

Fig. S4. (**A**) Implanted ectopic thymi generate T cells normally. FACS analysis of ectopic thymus implanted 5 months prior. (**B**) Total and $CD4^+$ cell numbers in the spleens of ATI and sham-operated mice 5 months prior. (**C**) Continuous transfer of

naïve $CD4^+$ T cells suppresses the age-dependent increase of $CD153^+$ SA-T cells. Naïve $CD4^+$ T cells (10^7 cells) from CD45.1 B6 mice were transferred into 5-9 month old CD45.2 B6 mice once a week for 3 months, and then the proportions of PD-1^+ $CD153^+$ T cells at the $CD45.2^+$ $CD4^+$ cell gate were analyzed. Control mice equally divided in terms of age distribution received PBS each time.